



EVALUATION OF SEISMIC RISK: APPLICATION TO BRIDGES AND VIADUCTS IN VENETO (ITALY)

P. Franchetti¹, M. Grendene¹, C. Modena¹, D. Slejko², F. Bergo¹

SUMMARY

As part of the project of the Gruppo Nazionale per la Difesa dai Terremoti “Scenarios of seismic damage in Friuli and Veneto”, the results are presented of a preliminary campaign to evaluate seismic risk to bridges and viaducts in the Veneto Region (Italy). The risk is quantified by means of fragility curves obtained by two different procedures: the first based on the US Hazus methodology, the second on a numerical determination of the curves. As the results of the Hazus application are based on US structural types they can only be indicative. To overcome this, analytical fragility curves were obtained specifically for some Italian types using both “push-over” (non-linear static) analysis and non-linear dynamic analysis. The results agree with those in the literature because “push-over” analysis, also proposed by ATC, underestimates the plastic displacements at the top of the piers: the fragility curves move to the right against safety, in spite of the non-linear dynamic analysis. On the other hand, the main advantage of the simplified procedure is the execution speed of a static analysis.

INTRODUCTION

For bridges and viaducts in an area at risk of earthquakes it is not sufficient to define their operating efficiency - this must also be flanked by a judgement on their seismic vulnerability, especially in the light of the ordinance 3274 of 20 March 2003 [1].

The necessity of dealing with many structures [2] [3], often with very limited means, necessitates the application of a rapid method, sufficiently simple to apply and that provides reliable results, in order to draw up a map that can immediately identify the structures at risk in the case of a seismic event.

The aim of this work was to construct and compare fragility curves obtained with different methods from the literature. These represent the probability of overcoming a determined damage level following an earthquake: the final judgement is therefore expressed in probabilistic terms.

Without any sure knowledge on a possible earthquake, the intensity of the tremors and their frequency can only be forecast statistically by studying past events. The fragility curves represent the probability of excess damage depending on the intensity of the earth tremors.

¹ Dipartimento di Costruzioni e Trasporti, University of Padua, Italy

² Istituto di Oceanografia e Geofisica Sperimentale, Trieste, Italy

The risk variables include the mechanical characteristics of the structure as well as the type of earthquake. Although the former are less uncertain, the properties of the concrete and/or steel in an existing structure can never be defined precisely.

BRIDGES ANALYSED

The analyses were conducted on the following bridges in the Belluno-Treviso area:

Lake Santa Croce Bridge, in the Santa Croce del Lago area (province of Belluno), has three spans max 20m in p.r.c. resting on piers in r.c. Deck width is 10m.

Botteon Viaduct, in the Fadalto area (province of Treviso), has six spans max 24m in p.r.c. resting on piers in r.c. Deck width is 11.5m.

San Vendemmiano Flyover, in the San Vendemmiano area (province of Treviso), has 17 spans max 12m in p.r.c. resting on piers in r.c. Deck width is 10m.

Quero Bridge over the River Piave, in the Quero area (province of Belluno), has 12 spans max 34.5m in p.r.c. resting on piers in r.c. Deck width is 10m.

Fener Bridge over the River Piave, in the Fener area (province of Treviso), has 25 spans max 24.75m in p.r.c. resting on piers in r.c. Deck width is 9m.

Hypothesising a given degree of uncertainty over the properties of the materials used, the analyses were conducted using R_{ck} 26, 28, 30, 32, 34 for the concrete and f_{yk} 420, 430, 440 for the steel. The behaviour of the materials is considered elastic-perfectly plastic.

REGIONAL SEISMIC RISK IN TERMS OF PGA

Peak acceleration values of 0.1 g, 0.2 g, 0.3 g, 0.4 g, 0.5 g and 0.6 g were considered for the studied sites, and response spectra to uniform risk were constructed for these acceleration values.

It is possible to construct the concise accelerogram with a spectral content extremely close to that described by the response spectrum to uniform risk. The stochastic vibrations approach [4] was used for this, according to which each periodic function (and so each seismogram) can be expanded with a series of sinusoidal functions of varying dimensions and phase. This method was formalised in the SIMQKE code [5] and has the following characteristics: 1) it calculates the function of spectral density intensity starting from an over-refined response spectrum chosen as target spectrum, and 2) it generates statistically independent accelerometric time-series compatible with the target response spectrum. In order to partially simulate the transient nature of real earthquakes, the stationary motion described by the series of sinusoids is multiplied by a function of deterministic intensity, which can assume a trapezoidal or exponential shape. The response spectrum is calculated for a whole series of damping values.

The response spectrum to uniform risk for the analysed sites (target spectrum), to be reproduced by means of the concise accelerogram, was defined using the 46 pairs of values (period, SA) which identify it, obtained from the probability calculation with the attenuation ratios of Ambraseys [6]. The SA values referring to rock were selected, and calculated taking the standard deviation of the attenuation ratio into account because the expected values are scattered around the average value which the standard deviation takes into account: the accelerogram to be constructed will thus represent a statistically precautionary situation. Different tests were done varying the number of iterations of adjustment to target spectrum and using different shapes for the intensity envelope function. Agreement with the target spectrum was good, apart from the oscillations not present in the probability spectrum, the construction of which had made over-refined.

ANALYSIS METHODS

The analysis methods examined included an approximate procedure described in the ATC-40 document [7] for calculating structural deformation caused by an earthquake. This procedure is considered approximate as it avoids a dynamic analysis of the inelastic system, substituting it by an analysis of a sequence of equivalent elastic systems. Each deformation value, belonging to the plastic branch of the initial system, corresponds to a different elastic system with a distinct period and viscous damping values. Reaching the point of intersection between the curve of capacity and curve of demand requires an iterative process, because the curve of demand of the ratio of viscous damping of the system is the function which changes at each iteration.

Chopra [8] showed that the results provided by the ATC procedures are incorrect as they are based on simplistic hypotheses, so they proposed changes. In particular, with reference to the “Capacity Spectrum Method” (CSM), criticism is made of the approximation in estimating the deformation caused by an earthquake as a sequence of linear equivalent systems, thus avoiding the analysis of the inelastic system. It is also noted that the simplified procedures do not always converge. Alternative procedures are therefore proposed which can be implemented numerically. For the construction of the diagram of demand, these procedures use the inelastic spectrum at constant ductility, instead of the elastic project spectrum used in the ATC-40 methods.

A parametric comparative analysis was first done between different analysis methods available in the literature. In particular the fragility curves were developed using the CSM proposed by ATC-40 [7] [9] [10] [11] [12] and those modified by Chopra [8] and non-linear dynamic analysis [11]. Although the CSM was proposed for the seismic evaluation of buildings and not bridges, these analysis methods have also been used for bridge structures [11].

For comparing the different methods it was decided to use an idealised system made of a support embedded at the base and a mass at the top with the following characteristics:

rectangular section dimensions $B = 1.5\text{m}$, $H = 2\text{m}$

- height $L = 16\text{m}$
- distinct period $T_n = 1\text{ s}$
- elastic modulus $E = 31143\text{ N/mm}^2$
- displacement of the top at yield point $u_y = 2.56\text{ cm}$
- ratio between yield strength and weight $f_y/w = 0.103$

Procedures A and B of ATC-40 were applied first. The spectrum of demand was obtained from the elastic spectrum of Eurocode 8 [13], assuming a ground of type A.

The “push-over” curves necessary for defining the diagram of capacity were obtained using the SAP2000 finite elements code. The system was schematised with 8 “beam” elements of 2 m in length, each one embedded at the base and with the mass concentrated in the topmost node. The “push-over” force was applied to that node, and its displacement was taken as control value. To construct the curve it was necessary to define in the programme the properties of the hinge at the base, i.e. the value of the yield force and slope of the plastic branch, the elastic branch already having been defined by the section characteristics and the elasticity module. For simplicity a bilinear elastic-perfectly-plastic behaviour was set.

The curve obtained from this analysis represents the shearing at the base as a function of the displacement at the top. Table 1 reports a comparison of the results obtained following the various procedures.

It can be noted that: the simplified procedures proposed by ATC-40 underestimate the deformation required by the earthquake. But the error is small for systems with reduced ductility; the comparison between the various simplified and modified procedures, which differ by the way in which the spectra are reduced as a function of the ductility, has demonstrated that the differences are small for values of the

distinct period around 1 sec; the modified procedures tend to overestimate the deformations and act in support of safety.

ATC - 40		CHOPRA-GOEL graphics			CHOPRA-G. no.			RHA
proc. A	proc. B	proc.A K-N	proc.A q=μ	Proc.B q=μ	NH	KN	VFF	
4.8	4.6	6.9	7.1	7.5	7.5	7.3	6.3	5.2

Table 1 Comparison between the displacements obtained at the top of the pier in centimetres, using the simplified procedures, those modified and non-linear dynamic analysis (RHA). NH = Newmark-Hall, KN = Krawinkler-Nassar, VFF = Vidic-Fajfar-Fischinger [8].

FRAGILITY CURVES

Introduction

Fragility curves are an efficient and intuitive tool for evaluating the seismic vulnerability of bridges and viaducts. They are made up of a series of diagrams representing the magnitude of the earth tremors expressed in a peak of horizontal acceleration (PGA) in the x axis, and the probability of surmounting the damage level to which the curve refers in the y axis. The probabilistic nature of the problem is made necessary by the randomness of some of the variables, such as the intensity of the tremors to be expected and the values of effective resistance of the bridge components. Fig. 1 [14] stresses these uncertainties, showing that the diagrams of demand and capacity can be obtained through the use of probability distributions. The obvious conclusion is that the performance level required is not represented by a point but by an interval of intersecting points.

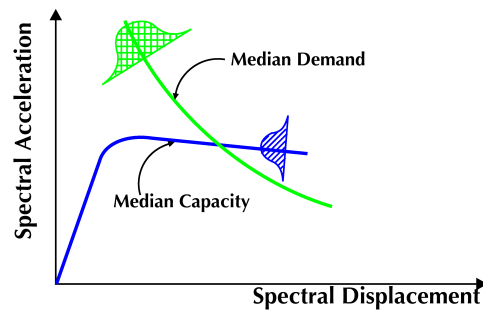


Fig. 1. Convergence between curve of capacity and curve of demand: the casualness and/or uncertainty of the structural behaviour and seismic response are stressed.

The structural capacity and seismic demand are random variables which adapt to a probabilistic distribution of the log-normal type, and so their intersection point can also be represented by a log-normal type distribution. From this representation can be obtained the density of cumulative probability, which takes the name “fragility curve”. Two parameters are necessary to describe this curve: the average value (value with a 50% probability of occurring) and the standard deviation. The equation that describes the density of cumulative probability is as follows:

$$F(S_a) = \Phi \left[\frac{1}{\beta_c} \ln \left(\frac{S_a}{A_i} \right) \right] \quad (1)$$

where Φ is the log-normal distribution function; S_a is the spectral acceleration; A_i is the median of the expected value of spectral acceleration necessary to cause the damage level demanded; β_c is the

normalised and log-normal standard deviation that incorporates the aspects of uncertainty and casualness of the capacity and demand as mentioned above.

The value of this latter parameter has been studied by different authors: the value proposed in Mander et al. (1999) is $\beta_c=0.6$, while that used in the HAZUS system [15] is $\beta_c=0.4$.

The median values A_i of the spectral acceleration necessary to cause a given level of damage can be determined, after having defined the levels of damage, taken approximately as multiples of the limit values of elasticity.

First approach for constructing the fragility curves: the Hazus method

The reason for developing this method was to be able to construct the fragility curves of a specific bridge using a limited number of data and avoid complex structural analyses. These suppositions make it possible to evaluate a large number of structures in a short time.

Only three types of data are necessary to develop the curves: 1) data relating to the geometric-structural characteristics of the bridge and its geographical location; 2) data on the forecast earthquake for that site; 3) information on the type of ground where the structure is built.

This method bases the construction of the curves on a prior division of bridges into different categories according to type, i.e. their geometric-structural characteristics.

Construction of the fragility curve of a specific bridge is done by adapting the curve for a “standard bridge”, i.e. a bridge long enough to be able to disregard the three-dimensional effects present. For the “standard bridges” belonging to each category, the PGA values necessary to cause determined damage levels (a_1, a_2, a_3, a_4) are obtained. These PGA values are then modified with the use of factors that take into account the angle of incidence (K_{skew}) and three-dimensional effects (K_{3D}) related to the specific bridge.

The PGA values which define the curve of the “standard bridge” are contained in a table, with the varying of the structural type showing the difference between structures designed using anti-seismic criteria and those not.

The following steps are taken to construct the curve of a specific bridge:

identification of the bridge characteristics: location, structural type according to predefined classes, number of spans (N), angle of incidence (α), deck width (W), total length (L), maximum length of the spans (L_{max});

evaluation of the type of ground where the structure is built;

calculation of the three factors which modify the standard curve.

Assuming a standard deviation value which identifies the data dispersal equal to $\beta=0.4$ delineates the fragility curves. The figures show examples of the fragility curves of some bridges.

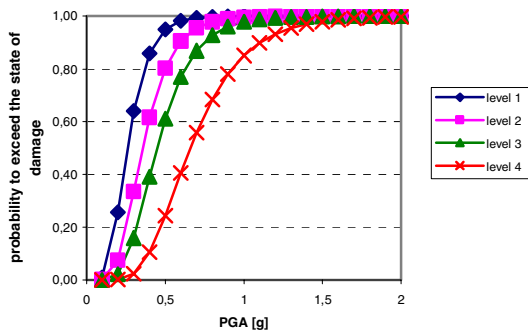


Fig. 2. Fragility curves for the different damage states of the San Vendemiano flyover.

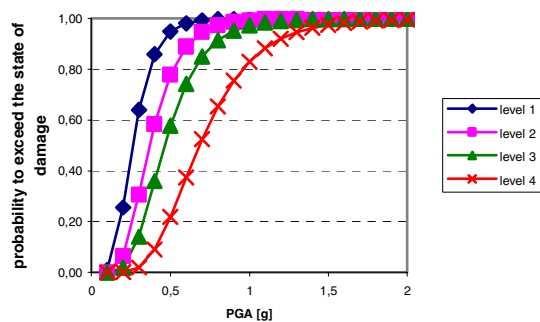


Fig. 3. Fragility curves for the different damage states of the Botteon viaduct.

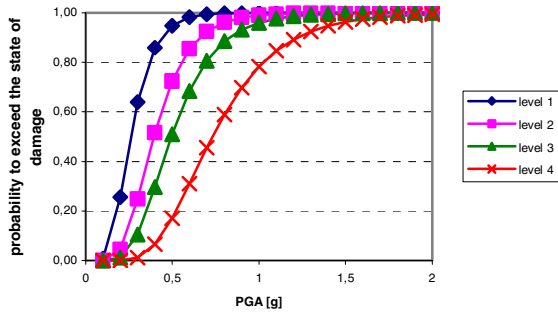


Fig. 4. Fragility curves for the different damage states of the bridge over Lake Santa Croce.

Construction of the fragility curves through non-linear static analysis

Fragility curves were obtained analytically for the same bridges as those analysed in the previous section using the displacements caused to the structure by an earthquake.

The method adopted for constructing the curves is based on one in the literature [9], and considers both the variability of the forecast earth tremors and the characteristics of the materials used in the structure.

Given the type of bridges analysed, the pier was considered as the element characterising bridge vulnerability, which is schematised as a vertical support embedded at the base and free at the top.

To take account of any possible difference in performance of the concrete and steel actually used in the structure compared to those used in the test, different possible resistances of the materials were considered. Hypothesising five different combinations of resistance of the materials for each bridge, five “push-over” curves were obtained, which represent the possible structural performances.

These “push-over” curves were obtained using the SAP2000 finite elements code, hypothesising the formation of a plastic hinge for rotation at the base of the pier. The model used was therefore constituted of “beam” elements with a plastic hinge at the base (specific to non-linear static analysis) and a mass at the top, equal to the mass of the deck which competes to the pier.

The five curves allowed, by changing the variables, the curves of capacity necessary for the evaluation of “point performance” to be obtained. To express the forecast tremors in probabilistic terms, 30 accelerograms were used, divided into 6 groups based on the PGA value (0.1g; 0.2g; 0.3g; 0.4g; 0.5g; 0.6g). To determine the “point performance” using the CSM proposed by the ATC, the relative response spectrum was obtained from each accelerogram. Every PGA value therefore made available 5 spectra from which it was possible to calculate the average spectrum and standard deviation from the average spectrum. From the intersection of these spectra with the curves of capacity of the pier, appropriately reduced following method B proposed by ATC-40, three points of capacity were obtained for each bridge and for each of the resistance values of the chosen materials. The values thus obtained were called $\bar{S}_d(a)$ for the intersection of the diagram of capacity with the average spectrum m and $\bar{S}_d(a) + \sigma_d^+(a)$, $\bar{S}_d(a) - \sigma_d^-(a)$ for the intersection with $m + \sigma$ and $m - \sigma$, respectively.

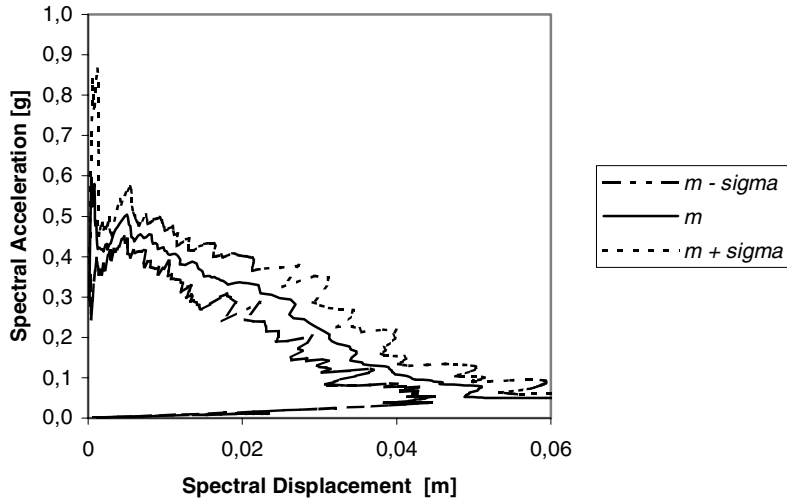


Fig. 5. Spectra of demand in ADRS format for a PGA value of 0.3g: spectrum average and spectrum average \pm deviation standard.

Usually the $\sigma_d^+(a)$ and $\sigma_d^-(a)$ values do not coincide, so in order to pass to the probability distribution the average value $\bar{S}_d(a)$ and standard deviation $\sigma_d(a)$ are taken, redefined as:

$$\sigma_d(a) = \sqrt{\sigma_d^+(a) \cdot \sigma_d^-(a)} \quad (2)$$

The parameters necessary for the lognormal distribution can then be obtained from the following equations

$$\bar{S}_d(a) = c(a) \exp\left[\frac{\{\zeta(a)\}^2}{2}\right] \quad (3)$$

$$\{\sigma_d(a)\}^2 = \{\bar{S}_d(a)\}^2 \left[\exp\left(\{\zeta(a)\}^2\right) - 1 \right] \quad (4)$$

The next step in creating the curves was to set the damage levels through the displacement values. In this study it was decided to set four levels, identifying them as multiples of the displacement value at yielding (value directly correlated with the ductility). The four values are: $d_1 = u_y$; $d_2 = 1.5u_y$; $d_3 = 2u_y$; $d_4 = 3u_y$;

These elements having been defined, it was possible to calculate the probability of the j-th bridge, i.e. a predetermined bridge with the characteristics of the j-th material, to equal or surmount a damage level identified by d_l using the following equation:

$$P_j[S_d(a) \geq d_l] = P_j(a, d_l) = 1 - \Phi \left[\frac{\ln\left(\frac{d_{l,j}}{c_j(a)}\right)}{\zeta_j(a)} \right] \quad (5)$$

where $c_j(a)$ and $\zeta_j(a)$ are extrapolated from equations (3) and (4). The index j indicates that parameters d_l , $c_j(a)$ and $\zeta_j(a)$ depend on the bridge being considered (intended as the same bridge physically, but with different characteristics of the materials). Different probability values were thus obtained with the varying of the material characteristics, and the final fragility value was extrapolated from an arithmetic mean as follows:

$$F(a, d_l) = \frac{\sum_{j=1}^K P_j(a, d_l)}{K} \quad (6)$$

where K is the number of variations of material considered. The fragility curves of some studied bridges are reported as examples:

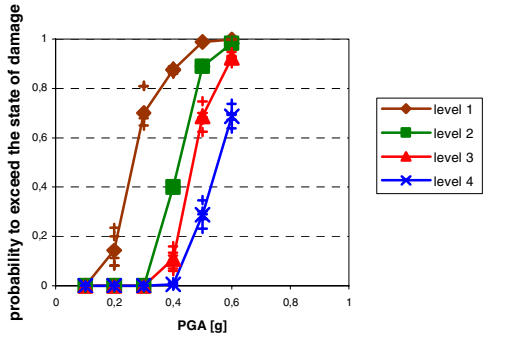


Fig. 6. Fragility curves of the San Vendemiano flyover for the different damage levels: points determined with procedure B of ATC-40

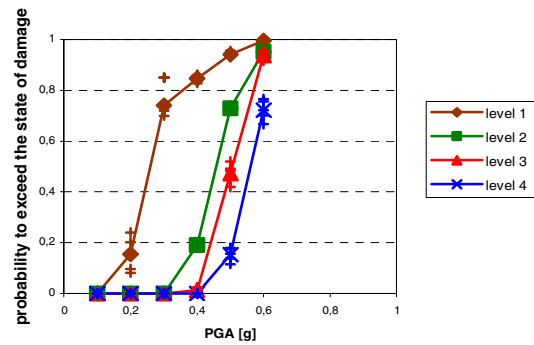


Fig. 7. Fragility curves of the Botteon viaduct for the different damage levels: points determined with procedure B of ATC-40

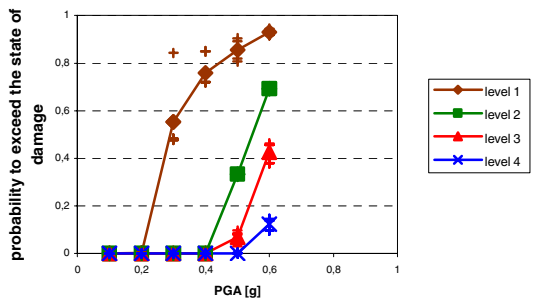


Fig. 8. Fragility curves of the bridge over Lake Santa Croce for the different damage levels: points determined with procedure B of ATC-40

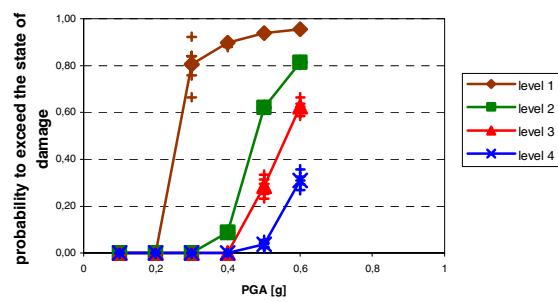


Fig. 9. Fragility curves of the Quero bridge over the River Piave, for different damage levels: points determined with procedure B of ATC-40

Construction of the fragility curves: non-linear dynamic analysis

Equation (6) was also used to determine the fragility curves with non-linear analysis in a time history. The displacements were obtained directly from the SAP2000 finite elements programme where a more suitable model for this type of analysis had previously been created. This model is very similar to the static equivalent analysis one, but with the insertion of a non-linear element of the “non-linear link” type, which simulates the formation of the plastic hinge for rotation following the earth tremor generated directly by the accelerogram. The characteristics of the non-linear element are introduced according to the type of concrete and amount of reinforcement in the section, hypothesising an elastic-plastic behaviour for the sake of simplicity. From the non-linear analysis for each of the 30 available accelerograms, and for the

different material values, the maximum displacements required were obtained, grouped according to the PGA value to which they refer. For each group it was thus possible to determine the values of $c_f(a)$ and $\zeta_f(a)$ to insert in (5), maintaining the values of $d_{i,j}$ unvaried with respect to CSM. The final fragility value for each PGA was lastly obtained by again applying equation (6).

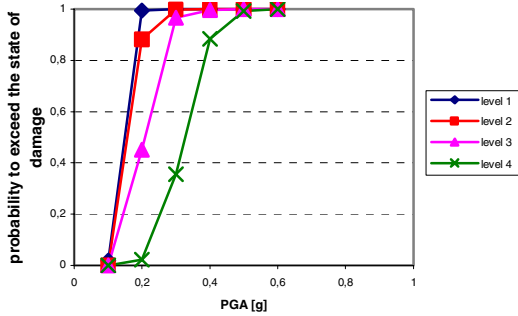


Fig. 10. Fragility curves of the San Vendemiano flyover for the different damage levels: points determined by dynamic analysis in time history.

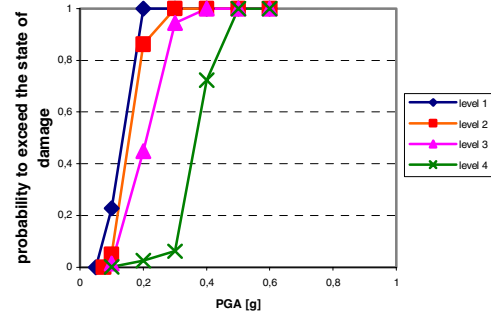


Fig. 11. Fragility curves of the bridge over Lake Santa Croce for the different damage levels: points determined by dynamic analysis in time history.

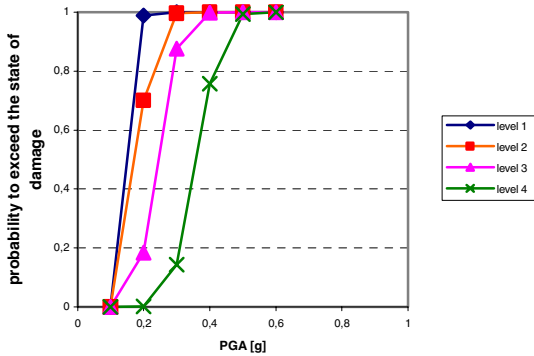


Fig. 12. Fragility curves of the Botteon viaduct for the different damage levels: points determined by dynamic analysis in time history.

CONCLUSIONS

These applications confirm the limitations inherent in the simplified procedures proposed by ATC-40. Despite being fast and easy to understand for evaluating the deformation caused by an earthquake, they are not sufficiently accurate, leading to errors of underestimation of as much as 60%. In addition, procedure A does not converge in many cases, so it would not be possible to adopt it as an evaluation method within a system of bridge management. These errors are caused by the substitution of the real elastic-plastic system with a series of linear systems, thus leading to iterate on overly high damping values (up to 40%). It should in fact be considered that transformation of the response spectra in the pseudo acceleration-displacement format is possible with the proviso that a simplification is made which leads to minor differences for damping values of up to 20%, but not beyond.

The alternative proposed in Chopra [8] to iterate on the ductility value, instead of on that of the damping as laid down in ATC-40, provides more accurate results. This method is only possible using simplified response spectra, like that proposed in Eurocode 8 [13], which can be reduced according to the ductility.

For response spectra obtained as an integration of the accelerograms no reduction method depending on ductility is yet available, so it is not possible to iterate according to this.

The determination of the required displacements through non-linear dynamic analyses is always the most accurate, but requires a careful construction of the model to be analysed. Particular attention must be paid to the non-linear elements that simulate the formation of the plastic hinges.

As regards the fragility curves, the method proposed in HAZUS [15] is extremely fast and easy to apply. These characteristics are essential in a system of bridge management which plans the classification of many structures. However, this method was developed and calibrated according to US types, building methods and regulations.

The construction of the fragility curves, based on real accelerograms of the investigated area, is, without doubt, the most accurate procedure, despite the need for a large number of accelerograms. The preliminary nature of the study does not yet allow accurate evaluations of the forecast damage to be obtained. Nevertheless, if only from the comparison between the results obtained between bridges of a similar type and prior to conducting more extended analyses, it is already possible to observe the efficiency of the method for comparative evaluations between the calculated fragility curves.

ACKNOWLEDGEMENTS

We wish to thank the management authorities of the bridges examined, who very kindly provided the project documentation essential for the analyses of seismic risk.

REFERENCES

1. Ordinanza 3274 della presidenza del Consiglio dei Ministri del 20 marzo 2003.
2. Regione Lombardia-Direzione Generale Territorio e urbanistica, C.N.R.-Istituto di Ricerca sul Rischio Sismico. "Vulnerabilità Sismica delle infrastrutture a rete in una zona campione della regione Lombardia", 2001.
3. Web site: <http://ibrid.dic.unipd.it>.
4. Vanmarcke E.H. "Structural response to earthquakes". In Lomnitz C, Rosenblueth E. (eds). "Seismic risk and engineering decisions". 1976; Elsevier, Amsterdam Oxford New York, pp. 287-337.
5. Gasparini D.A, Vanmarcke E.H. "Simulated earthquake motions compatible with prescribed response spectra". Massachusetts Inst. Technol., 1976; publ. R76-4, 65 pp.
6. Ambraseys N. N, Simpson K. A, Bommer J. J. "Prediction of horizontal response spectra in Europe". Earth. Eng. Struct. Dyn., 1996; 25: 371-400.
7. Applied Technology Council (ATC). "Seismic evaluation and retrofit of concrete buildings". Rep. No. SSC 96-01: ATC-40, 1996; 1, Redwood City, California.
8. Chopra A, Goel, "Capacity-Demand-Diagram methods for estimating seismic deformation of inelastic structures". SDF systems, Pacific Earthquake Research Center, 1999.
9. Saxena, Deodatas, Shinozuka M, Feng M. "Development of Fragility Curves for Multi-Span Reinforced Concrete Bridges", 2000.
10. Deodatas, Shinozuka M, "Effect of spatial variability of ground motion on bridge fragility curves". 8th ASCE Specialty Conference on Probabilistic Mechanics and Structural Reliability, 2000.
11. Shinozuka M, Feng M. Q, Kim S.H. "Nonlinear Static Procedure for Fragility Curves Development". Journal of Engineering Mechanics, 2000; Vol. 126, No.12.
12. Shinozuka M, Grigoriu, Ingrassia, Billington, Feenstra, Soong, Reinhorn, Maragakis. "Development of Fragility Information for Structures and Nonstructural Components", 2000/b.
13. Eurocode 8: "Design provisions for earthquake resistance of structures".
14. Mander. "Fragility Curves Development for Assessing the Seismic Vulnerability of Highway Bridges", 1999.
15. HAZUS99 Technical Manual. "Direct Physical Damage to Lifelines-Transportation Systems". Chapter 7.